Charge Motions During the Photocycle of *pharaonis* Halorhodopsin

Krisztina Ludmann,* Grazyna Ibron,† Janos K. Lanyi,‡ and György Váró*

*Institute of Biophysics, Biological Research Center of the Hungarian Academy of Sciences, Szeged H-6701, Hungary; †Department of Physics and Biophysics, University of Agriculture and Technology, 10-957 Olsztyn, Poland; and ‡Department of Physiology and Biophysics, University of California, Irvine, California 92697 USA

ABSTRACT Oriented gel samples were prepared from halorhodopsin-containing membranes from *Natronobacterium pharaonis,* and their photoelectric responses to laser flash excitation were measured at different chloride concentrations. The fast component of the current signal displayed a characteristic dependency on chloride concentration, and could be interpreted as a sum of two signals that correspond to the responses at high-chloride and no-chloride, but high-sulfate, concentration. The chloride concentration-dependent transition between the two signals followed the titration curve determined earlier from spectroscopic titration. The voltage signal was very similar to that reported by another group (Kalaidzidis, I. V., Y. L. Kalaidzidis, and A. D. Kaulen. 1998. *FEBS Lett.* 427:59–63). The absorption kinetics, measured at four wavelengths, fit the kinetic model we had proposed earlier. The calculated time-dependent concentrations of the intermediates were used to fit the voltage signal. Although no negative electric signal was observed at high chloride concentration, the calculated electrogenicity of the K intermediate was negative, and very similar to that of bacteriorhodopsin. The late photocycle intermediates (O, HR′, and HR) had almost equal electrogenicities, explaining why no chloride-dependent time constant was identified earlier by Kalaidzidis et al. The calculated electrogenicities, and the spectroscopic information for the chloride release and uptake steps of the photocycle, suggest a mechanism for the chloride-translocation process in this pump.

INTRODUCTION

Halorhodopsin is a light-driven chloride ion pump in the cell membrane of halophilic archaea (Lanyi, 1990; Oesterhelt, 1995). As in the proton pump, bacteriorhodopsin, the photoisomerization of the all-*trans* retinal to the 13-*cis* form, initiates a photocycle that is associated with chloride ion translocation from the extracellular medium into the cytoplasm (Schobert and Lanyi, 1982; Oesterhelt and Tittor, 1989).

Aside from *salinarum* halorhodopsin in *Halobacterium salinarum* (Matsuno-Yagi and Mukohata, 1980) and *pharaonis* halorhodopsin in *Natronobacterium pharaonis* (Bivin and Stoeckenius, 1986), numerous other halorhodopsins have been reported in the extreme halophiles (Otomo et al., 1992; Soppa et al., 1993; Ihara et al., 1999). The amino acid sequences and three-dimensional structures of these different halorhodopsins exhibit considerable similarity to each other and to those of the bacteriorhodopsin (Blanck and Oesterhelt, 1987; Lanyi et al., 1990b; Otomo et al., 1992; Havelka et al., 1995). The similarity is greater in the transmembrane helical segments of the protein, primarily in the retinal binding pocket. Unlike bacteriorhodopsin, however, the halorhodopsins bind and transport chloride. In the presence of chloride, the absorption maximum of *pharaonis* halorhodopsin shifts toward the blue, revealing a binding constant of ~1 mM for the chloride ion (Scharf and Engelhard, 1994).

Received for publication 3 June 1999 and in final form 28 October 1999.

Address reprint requests to Dr. György Váró, Institute of Biophysics, Biological Research Center of the Hungarian Academy of Sciences, P.O. Box 521, Szeged H-6701, Hungary. Tel.: 36-62-432232; Fax: 36-62-433133; E-mail: varo@nucleus.szbk.u-szeged.hu.

0006-3495/00/02/959/08 $2.00

The transient absorption changes of *pharaonis* halorhodopsin indicate a photocycle similar to that of *salinarum* halorhodopsin (Scharf and Engelhard, 1994; Váró et al., 1995b). In both proteins, other than the chloride-transporting photocycle, determined at a saturating chloride concentration, a nontransporting cycle was observed when the chloride was replaced with sulfate. At intermediate chloride concentrations the photocycles could be decomposed into these two components. The dependency of their ratio on chloride displayed the same apparent binding constant as the binding of chloride ions to the proteins (Váró et al., 1995a). On the bases of spectral and kinetic analogy with bacteriorhodopsin, the intermediates in the transporting photocycle of *pharaonis* halorhodopsin have been named K, L, N, O, HR′, and HR. The main difference from the photocycle of *salinarum* halorhodopsin is that in the latter, probably for kinetic reasons, the O state does not accumulate (Váró et al., 1995c). The chloride photocycle of *pharaonis* halorhodopsin proved to have two chloride-dependent rate constants that were assumed to correspond to 1) the reverse of the chloride release step, and 2) the chloride reuptake step. The release and the uptake of chloride were thus associated with the N to O and the O to HR′ transitions, respectively (Váró et al., 1995a).

Measurement of electric signals on oriented samples is a well-known method for investigating light-activated retinal proteins. Different techniques have been used to achieve orientation of the protein-containing membrane patches: incorporation into lipid bilayer membranes (Bamberg et al., 1981; Butt et al., 1989), or oriented attachment of the membranes to a lipid-impregnated filter (Drachev et al., 1981; Kalaidzidis et al., 1998) or thin Teflon sheet (Holz et al., 1988). Although these techniques are very sensitive to the electric signals generated, they are inappropriate for

simultaneous measurements of absorption kinetics because the monolayer of protein-containing membranes on the supporting surface has very low optical density. At the same time, the attached sides of the membranes are not directly accessible to the bathing solution, and therefore there is a possibility for a large gradient to be built up across the membrane during excitation.

Another technique, involving oriented membranes encasted in acrylamide gel (Dér et al., 1985a), allows both absorption kinetics and electric signal measurements on the same sample, under the same conditions. This method eliminates all the problems of the earlier technique, except at high-salt concentration, where in the gels the sample resistance is low and the signal-to-noise ratio is decreased (Gergely et al., 1993; Ludmann et al., 1998a). The first electric signal measurements on bacteriorhodopsin in oriented samples indicated an already strong correlation between the photocycle transitions and the electric signal components (Keszthelyi and Ormos, 1980).

However suggestive, the results of these measurements cannot be interpreted simply in terms of the ion translocation steps. Displacements of charges originate from the movements of both the transported ion and charged amino acid side chains of the protein. Furthermore, the local dielectric constant inside the membrane is not well-defined. Accordingly, attempts to directly correlate the electric signals to the motions of the transported ion lead to oversimplification. To overcome this problem, the relative "electrogenicities" of the photocycle intermediates are defined as the changes in dipole magnitude of the intermediate relative to the unphotolyzed state of the protein (Trissl, 1990; Gergely et al., 1993). The electrogenicities of the bacteriorhodopsin intermediates have been determined (Dér et al., 1992), and their expected pH independence have been confirmed (Ludmann et al., 1998a).

The electric signal on *salinarum* halorhodopsin was first measured by attaching *salinarum* halorhodopsin-containing membrane fragments onto a positively charged planar lipid bilayer (Bamberg et al., 1984). The possibility of preparing *salinarum* halorhodopsin-containing oriented gel samples for electric signal measurements was later demonstrated on Tween-washed membranes (Dér et al., 1985b). *Pharaonis* halorhodopsin-containing membranes were recently attached to phospholipid-impregnated film and the electric signals were measured (Kalaidzidis et al., 1998). At high chloride concentration, the fast component of the photovoltage signal was attributed to the L intermediate. The later electrical signals could not be correlated with intermediates because the lack of absorption kinetics did not allow an exact fit to the photocycle, and the discharge time constant of the system limited the measurement to a few milliseconds. Another group measured chloride ion concentration-dependent responses to continuous illumination (Okuno et al., 1999). An attempt to interpret the relation of the electric signals to the photocycle was made by measuring the photocycle in suspension and the electric signal on film (Muneyuki et al., 1999). However, the 1-μs conversion time of their measurement did not allow resolution of the fast component of the signal. The discharge time constant gave a millisecond limit at the other end of the time scale, providing an active time window of less than three orders of magnitude. Nevertheless, it was concluded from these studies that only the appearance and disappearance of the N intermediate were electrogenic.

In the work we report here, oriented gel samples were prepared from *pharaonis* halorhodopsin-containing membranes. Electric signal and absorption kinetic measurements were made at different chloride concentrations. The time courses of the photocycle intermediates were calculated from the absorption kinetics; their fit to the electric signal allowed determination of the electrogenicity of the intermediates.

MATERIALS AND METHODS

The halorhodopsin gene from *N. pharaonis* was expressed in *H. salinarum* strain L33, and halorhodopsin-containing membranes were prepared as described earlier (Váró et al., 1995b). Before sample preparation the membrane suspension was centrifuged in 100 mM NaCl, 10 mM MES, pH 6. The oriented gel samples were prepared by polymerizing the gel around the membrane suspension in the presence of an external orienting field, following the procedure described earlier (Dér et al., 1985a). The samples were exhaustively washed with 1 M NaCl, 10 mM MES, pH 6. The sodium ion concentration of the measurement solutions was kept approximately constant by diluting the 1 M NaCl with 0.5 M Na_2SO_4. Before measurements, the gel samples were washed thoroughly and kept for several hours in the bathing solution to equilibrate the system. A temperature-controlled sample holder was used to keep the measurement temperature constant at 20°C.

Flash excitation at 532 nm was performed with a frequency-doubled Nd-YAG laser (Continuum, Surelite I-10). Absorption kinetic signals were recorded at 500, 590, 620, and 640 nm, in the time interval between 100 ns and several seconds. The earlier-established photocycle model of *pharaonis* halorhodopsin (Váró et al., 1995a) was fitted with the RATE program as described elsewhere (Ludmann et al., 1998b) and gave the time courses of the intermediates.

Electric signals were measured on a set-up described previously (Gergely et al., 1993), with the modification that a very low-noise homemade current preamplifier was used. Each measurement involved averaging 200 to 400 signals. The current signal and its integral, the voltage, were reproducible in the time interval from 100 ns to 20 ms. The electrogenicities of intermediates were calculated by using the MATLAB program, version 4.2c (Ludmann et al., 1998a).

RESULTS

The electric signals of *pharaonis* halorhodopsin-containing samples were ~1% of those of bacteriorhodopsin (Fig. 1, *A* and *B*), even though the amplitudes of the absorption changes in the visible were comparable (not shown). The discrepancy stems from the very small extent of orientation of the membranes. The halorhodopsin-containing membrane forms closed vesicles, in contrast with the bacteriorhodopsin-containing open purple membrane sheets. During sample preparation, when the suspension is mixed with the

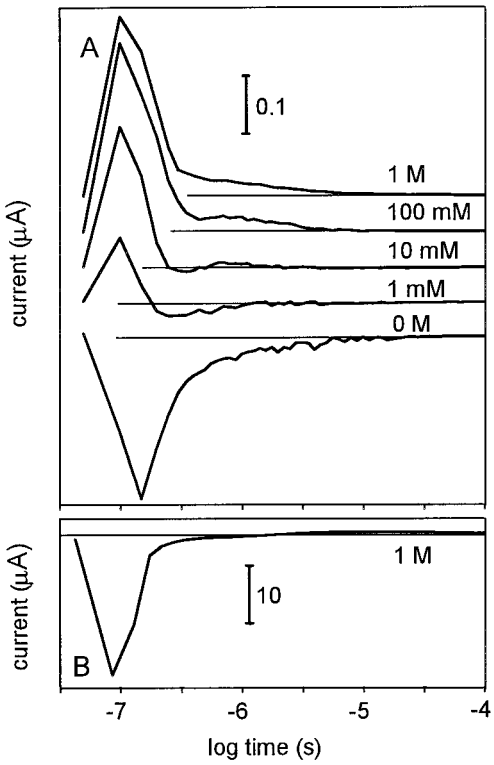

FIGURE 1 Laser-flash induced electric current measured for *pharaonis* halorhodopsin at different chloride concentration (*A*) and on bacteriorhodopsin (*B*). The sodium ion concentration of the solution was kept constant by diluting 1 M NaCl with 0.5 M Na_2SO_4. The measurement temperature was 20°C. The halorhodopsin signal was ~1% of that corresponding to bacteriorhodopsin.

acrylamide monomer solution, before orientation the vesicles could undergo partial opening due to the osmotic shock. Probably, only these opened vesicles were oriented and contributed to the electric signals. After the laser flash, the positive electric signal measured in 1 M NaCl (Fig. 1) could be identified as a positive charge moving toward the extracellular surface, or a negative charge moving toward the cytoplasm of the cell. This signal is opposite to the fast electric signal measured on bacteriorhodopsin, in which it arises from the isomerization of the retinal. The positive direction is the same as the translocation of the chloride ions across the membrane that will occur on a much slower time scale. Indeed, the sign of the photovoltage that develops from the transport (see below) is in this direction; i.e., the same direction as with bacteriorhodopsin, and suggests that when prepared with the same sign of orienting electrical field, the net orientation of these membranes is the same as purple membranes.

The current signal exhibited pronounced chloride concentration dependence (Fig. 1 *A*), varying from a positive signal at high chloride concentration to a negative one at zero chloride, when only sulfate was present in the solution. Plots of the amplitudes corresponding to 0.1 and 1 μs after the laser excitation as functions of chloride concentration (Fig. 2) could be fitted with a titration curve. The dotted line shows the same 0.75-order binding with a dissociation constant of 1 mM chloride as the earlier spectroscopic titrations (Scharf and Engelhard, 1994; Váró et al., 1995b). The shapes of the current signals at intermediate chloride concentrations suggest that they are the weighted sums of the high-chloride and the no-chloride electric signals. This is demonstrated by comparison of the 10- and 1-mM signals (Fig. 3, *solid line*) with calculated mixtures of the two limiting signals, with a ratio determined from the titration curve in Fig. 2 (Fig. 3, *dotted lines*).

Because the electric signal of *pharaonis* halorhodopsin is very small, the voltage signal was reliably reproducible only up to 20 ms (Fig. 4). At longer times even the very small baseline drift of the current introduced large errors in the time integral. In the usable time interval the discrepancies between different measurements were within ±5%. The voltage signals presented in Fig. 4 are the averages of several measurements. In the following we describe our investigations of the high-chloride concentration signals and how they yielded the desired information about the electrogenicities of the intermediates of the chloride-transporting photocycle. The absorption kinetic measurements of the gels were made at four wavelengths (Fig. 5 *A, solid lines*). These signals were fitted to the earlier published photocycle model (Váró et al., 1995b) (Fig. 5 *A, dotted lines*):

$$K \Leftrightarrow L \Leftrightarrow N \Leftrightarrow O \Leftrightarrow HR' \Rightarrow HR \qquad (1)$$

The extinction coefficients of the intermediates at the measured wavelengths were taken from the literature (Váró et al., 1995b). The resulting time-dependent concentrations of the intermediates are shown in Fig. 5 *B*. Consistent with the chloride dependencies of the photocycle steps described

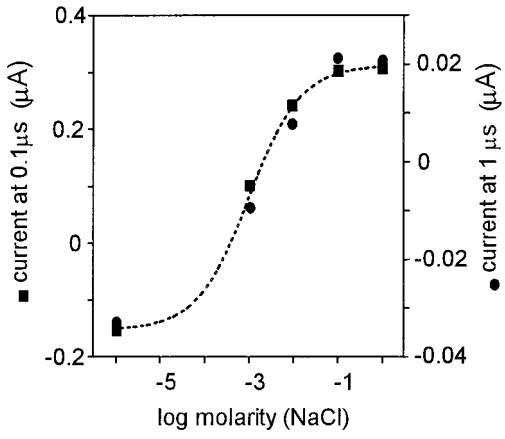

FIGURE 2 Changes in the amplitudes of the signals shown in Fig. 1 *A*. ■, Amplitude measured at 0.1 μs after photoexcitation; ●, amplitude measured at 1 μs after photoexcitation. The dotted line is the titration curve corresponding to the 1 mM binding constant with 0.75 binding order, as determined earlier (Váró et al., 1995a).

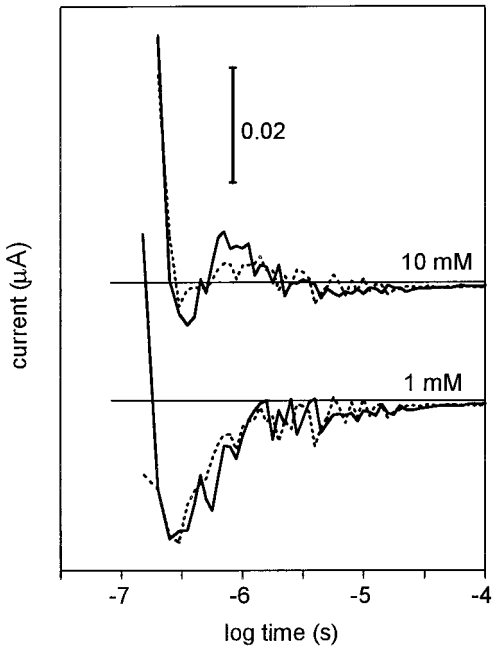

FIGURE 3 Current signals at two intermediate chloride concentrations (*solid lines*), and the linear combination of the signals at 1 M and 0 M chloride in the ratio determined from the titration curve in Fig. 2 (*dotted lines*).

earlier (Váró et al., 1995b), upon decreasing the chloride concentration from 1 M to 100 mM, significant changes were observed in the time course of the intermediates N, O, HR′, and HR (Fig. 6).

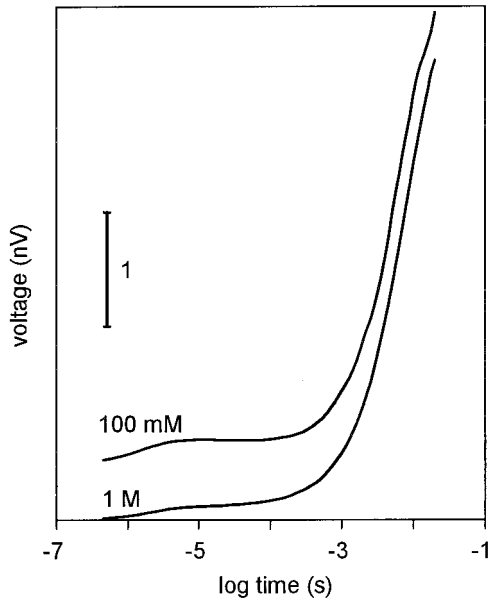

FIGURE 4 Voltage signal determined from the time integral of the current signal. The measurement conditions were similar to those in Fig. 1.

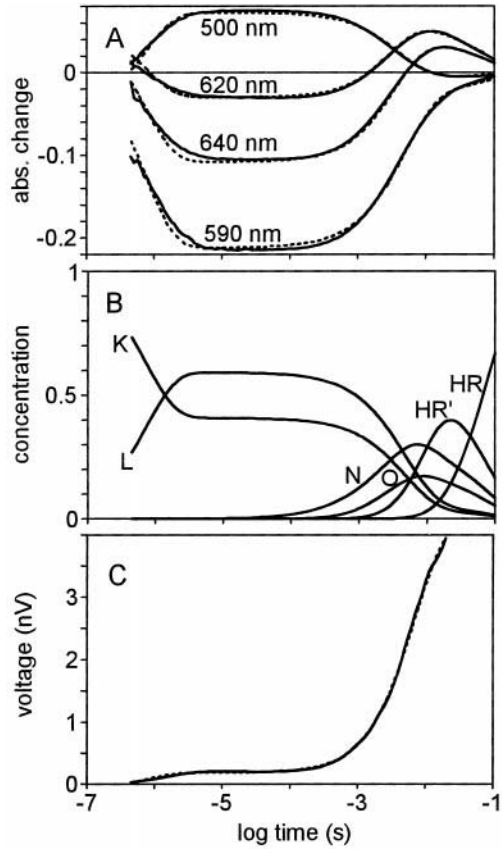

FIGURE 5 Absorption kinetic signals measured at different wavelengths (*A*; *solid lines*), and their fit to the photocycle model (*dotted lines*), the time course of the photocycle intermediates (*B*), and the fit of the voltage signal (*C*). Measurements were performed at 100 mM NaCl under the same conditions as in Fig. 1.

The best fit left considerable deviations in the microsecond time domain (Fig. 7 *A*). An improvement in the fit was achieved (Fig. 7 *B*) when two consecutive L intermediates were introduced:

$$K \Leftrightarrow L_1 \Leftrightarrow L_2 \Leftrightarrow N \Leftrightarrow O \Leftrightarrow HR' \Rightarrow HR \qquad (2)$$

With this modification, the χ^2 of the fit decreased from $6 \cdot 10^{-3}$ to $2.4 \cdot 10^{-3}$. From absorption measurements on *salinarum* halorhodopsin we had suggested a photocycle scheme with two L states (Váró et al., 1995c). Although from the electrogenicities of the intermediates we locate the extracellular-to-cytoplasmic switch at the L-to-N step (see below), a spectrally silent L_1-to-L_2 transition in *salinarum* halorhodopsin was assumed in the model by Oesterhelt (1995) to account for the switch event in the transport cycle.

The fit to the voltage signal was as for bacteriorhodopsin (Ludmann et al., 1998a). The electrogenicities of the intermediates were calculated with the relationship:

$$(t) = A \cdot \sum_i C_i(t) \cdot E_i$$

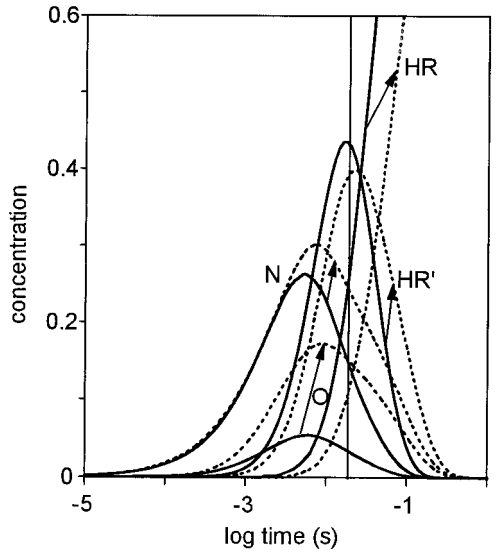

FIGURE 6 Time course of the intermediates in the second part of the photocycle, calculated from absorption kinetic signals measured at 1 M NaCl (*solid lines*) and at 100 mM NaCl (*dotted lines*). The vertical line shows the time limit where the electric signal measurement was terminated.

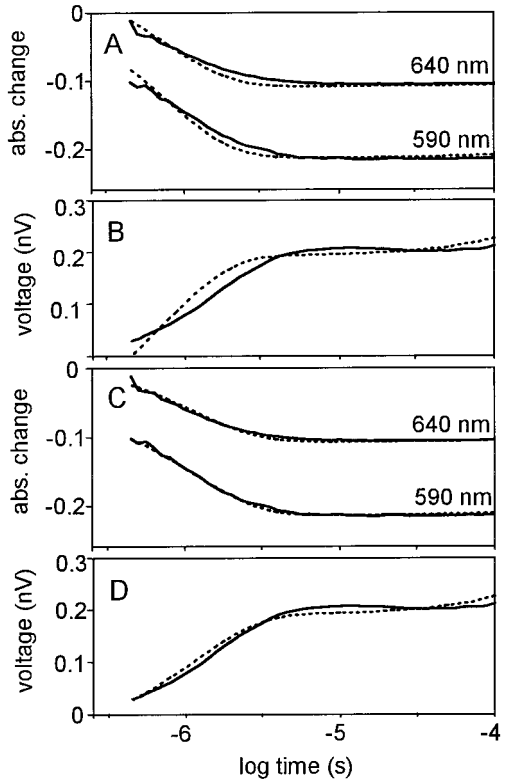

FIGURE 7 The early part of the measured absorption kinetics (*A* and *C*; *solid lines*) and voltage-signal (*B* and *D*; *solid lines*), shown in Fig. 5. Fit to the model with one L intermediate (*A* and *B*; *dotted lines*), and two L intermediates (*C* and *D*; *dotted lines*).

Where $U(t)$ is the voltage, A is a constant determined by the measurement conditions, $C_i(t)$ is the concentration, and E_i is the electrogenicity of intermediate i. The value of A is determined by the geometry (distance between the electrodes, size of the gel), the conductivity, and optical density of the sample, etc. The electrogenicity is the change in the dipole magnitude of the intermediate relative to the ground state (Trissl, 1990; Gergely et al., 1993). The fit to the first photocycle model (Fig. 5 *C*) gave the unexpected result of a negative electrogenicity for K. Careful inspection of the current signals in the ns domain also suggested the existence of a very fast negative component, because the first measured point of the 50-ns digitizer was consistently in the negative direction (not shown). Using the second photocycle model with two L intermediates, the fit improved in the microsecond time domain of the voltage signal (Fig. 7, *B* and *D*), giving the same electrogenicities: a negative one for intermediate K and equal electrogenicities for L_1 and L_2. Thus, we discuss only the values of the first model, although both models were fitted. The calculated electrogenicities for 1 M and 100 mM NaCl were very similar, even though the concentrations of the late intermediates displayed rather large changes (Fig. 6). The last column in Table 1 presents the relative electrogenicities, calculated in a similar way as for bacteriorhodopsin (Ludmann et al., 1998a), with the electrogenicity of intermediate K, as reference, taken as -1.

DISCUSSION

It should be emphasized that in these measurements only the component perpendicular to the membrane surface of the charge motions can be observed. The calculated voltage signal of halorhodopsin has a positive slow component (Fig. 4), similar to that of bacteriorhodopsin. This indicates that the membrane orientations in bacteriorhodopsin and halorhodopsin samples are the same: the cytoplasmic surface is directed toward the positive pole of the orienting electric field.

The electric signals, like the absorption changes, depend on chloride in two ways: 1) binding of chloride to the unphotolyzed state determines whether the photocycle is of the chloride-transporting kind or not, and 2) binding of chloride during the photocycle determines the rate of some steps of the chloride-transporting photocycle. The chloride

TABLE 1 Electrogenicities of the *pharaonis* halorhodopsin photocycle intermediates

Intermediate	Electrogenicity (μV)	Relative electrogenicity
K	−0.12	−1
L	0.32	2.7
N	2.13	17.7
O	5.35	44.6
HR′	5.1	43
HR	5.22	43.5

ion concentration dependence of the fast electric signal (case 1, Fig. 2) was similar to that determined earlier for the spectral shift of the ground-state spectrum and the absorption change determined at different wavelengths (Váró et al., 1995a). The rise of the current signal measured at high chloride concentration was fast (within 50 ns, the fastest conversion time of the transient digitizer, in Fig. 1 *A*, *trace* 1 M). Its decay was multiexponential. The fast-decaying component corresponds to the RC of the measuring circuit, while the slower one correlates with the K-to-L transition of the photocycle. The negative current signal measured in chloride-free solution appeared slower and its decaying part was not RC-limited. Its multiexponential course followed the time constants of the photocycle as measured by absorption in the visible (not shown).

The quality of the fit to the absorption kinetic measurements and the time course of the concentrations of the intermediates (Fig. 5) were similar to those published earlier (Váró et al., 1995b). Upon changing the chloride concentration of the bathing solution from 1 M to 100 mM, the transient accumulation of K and L varied by only a few percent (not shown), but considerable concentration rearrangements occurred in the second part of the photocycle (case 2). The maximum concentrations of intermediates N, O, HR′, and HR shifted toward longer times. The amount of O increased about threefold, and a small increase was observed in the accumulation of N. The HR′ and HR contents of the photocycle decreased before the time point where the electric signal measurement was terminated (Fig. 6, *vertical line*).

Similarly to the bacteriorhodopsin photocycle, in the microsecond time domain the fit was improved by the introduction of a second L intermediate (compare Fig. 7, *A* and *C*) (Zimányi and Lanyi, 1993; Gergely et al., 1993). Although we have no experimental evidence for the existence of the two L intermediates, a plausible explanation could be that the charge motion during the appearance of intermediate L_1 following retinal isomerization could result in structural distortion inside the protein. This distortion could relax without significant charge rearrangement, and result in L_2 with the same spectral and electric properties as those of L_1, but the decay of K will be affected.

The photovoltage signal up to several milliseconds appears very similar to that measured with a phospholipid-impregnated colloidal film (Kalaidzidis et al., 1998). In the film measurement there is a breakdown of the signal at several milliseconds due to the discharge time constant of the system. For the oriented gel, the measurement time period was one order of magnitude longer. The fit of the voltage signal involved an error of $\pm 2\%$ (Fig. 5 *C*), with the largest deviation in the microsecond time domain (Fig. 7 *B*). The introduction of the two L intermediates improved the fit (Fig. 7 *D*), and resulted in almost the same electrogenicities for the intermediates as in the previous model (not given). Despite the significant changes in the transient concentrations of intermediates in the second part of the photocycle, the fit of the electric signals gave almost identical electrogenicities at two different chloride concentrations tested. The average of them is given in Table 1.

The negative value of the calculated electrogenicity of the K intermediate is strikingly similar to that for bacteriorhodopsin. As both photocycles are initiated by an absorbed light quantum, and the first step is the photoisomerization of the retinal from the all-*trans* to the 13-*cis* conformation, the similar negative electrogenicities demonstrate that this event occurs in both proteins with the same charge separation. The apparent absence of this negative signal in the signal traces for *pharaonis* halorhodopsin can be explained by the fact that at the time-resolution of the transient digitizer (50 ns) the K intermediate is already formed and has began to decay to L, giving a positive current. Unlike K, the electrogenicity of intermediate L is different from that for bacteriorhodopsin. It appears that after K another process, different from the one in bacteriorhodopsin, occurs. In the proton-pumping bacteriorhodopsin, L still has negative electrogenicity, whereas in halorhodopsin it is positive. Up to 0.1 ms, the intermediates K and L remains in equilibrium, and the electric signal displays a plateau. It starts to increase sharply when intermediate N is formed. This determines the rather large electrogenicities of the late intermediates. Although the first two electrogenicities reveal only small charge rearrangements in the direction of the membrane normal, the L-to-N and N-to-O transitions are the main charge transfer steps, as suggested also by the photocycle model (Váró et al., 1995a), and the results of Muneyuki et al. (1999). The equality of the electrogenicities of O, HR′, and HR indicate that the transitions involving these intermediates do not involve appreciable charge shifts inside the protein. The chloride ion concentration dependencies of the photocycle steps have already revealed that the N-to-O and O-to-HR′ transitions are the chloride release and uptake steps, respectively (Váró et al., 1995a). The large red-shift of the maximum of the O state relative to the N state had suggested that in the N-to-O step, when the retinal reisomerizes to all-*trans* (Váró et al., 1995a), the bound chloride moves away from the immediate neighborhood of the Schiff base. The electrogenicity of the reaction indicates that this movement occurs inside the protein, and its direction is toward the cytoplasmic side. The chloride ion released to the cytoplasmic side during this reaction may be the same chloride that moved, or another chloride ion already bound near the cytoplasmic surface. In contrast to these events, the uptake of chloride from the extracellular surface, in the O-to-HR′ reaction that follows, is not accompanied by an electrical signal. It indicates that the chloride binds close to the protein surface. This is a paradox. The blue-shift of HR′ relative to O indicates that the binding of chloride affects the retinal Schiff base, yet one would expect that the entry of chloride to the vicinity of the Schiff base would generate an electrical signal. Long-range interaction between the

extracellular surface and the Schiff base, such as found in bacteriorhodopsin (Balashov et al., 1996) might be the explanation of the apparent contradiction.

Based on the knowledge accumulated in the literature and the results presented above we suggest a tentative mechanism for the chloride ion translocation process during the *pharaonis* halorhodopsin photocycle. Ion-pumping proteins must undergo a conformation change during their function. This should occur before the ion release and is probably accompanied by charge motion, involving a partial translocation of the transported ion. In this way the accessibility of the transported ion can change from one side of the membrane to the other. In the HR state, halorhodopsin binds chloride with high affinity, probably close to the extracellular surface of the membrane. In the *salinarum* halorhodopsin, at least, the binding site is presumed to be close to the extracellular surface and controlled by the positive charge of Arg-108 (Lanyi et al., 1990a; Braiman et al., 1994; Rüdiger and Oesterhelt, 1997). Upon absorption of a light quantum, the retinal is isomerized from all-*trans* to 13-*cis*, passing to the K intermediate with a small negative electrogenicity. The isomerization results in distortion of the retinal surroundings. Relaxation, with some charge rearrangement, leads to the L intermediate with a positive electrogenicity. Time-resolved resonance Raman spectroscopy shows that during this process the chloride ion moves closer to the Schiff base (Gerscher et al., 1997). After a rather long equilibrium period, in the transition to the N intermediate the chloride ion moves from the extracellular region inside the protein. At the same time, the protein changes its conformation, permitting ion accessibility toward the cytoplasm. This step has a rather large positive electrogenicity that may originate either from the movement of the chloride or the structural shift of the protein. In the latter case, however, we would expect negative electrogenicity in a later step, during recovery of the protein, and this is not seen. During the N-to-O transition the chloride ion moves across the protein, accompanied by a large electrogenicity change, and a chloride is released to the cytoplasmic surface. After the release step, during the O-to-HR′ transition, another chloride ion is bound on the extracellular side of the membrane and the protein relaxes back to the initial HR state, resetting the ion pump for the next cycle. The last two steps, the chloride binding and the reset of the protein to the original ground state, occur without large charge rearrangements perpendicular to the membrane surface. This model, supported by photocycle and photoelectric measurements with *pharaonis* halorhodopsin, resembles, at least qualitatively, the one suggested from the effects of site-specific mutations of residues at various locations in *salinarum* halorhodopsin (Rüdiger and Oesterhelt, 1997).

Even at its maximum, the O intermediate accumulates only to an extent of $<20\%$, yet the chloride-dependent transitions are the O-to-HR′ forward and the O-to-N reverse reactions (Váró et al., 1995a). However, when the fit of the voltage signal was effected by excluding intermediate O from the model, the error of the fit was much larger (not shown). The small amount of O, and its electrogenicity being equal to those of HR′ and HR, can explain why no chloride-dependent component could be detected by Kalaidzidis et al. (1998). Their electric signal reflects the real processes occurring in the photocycle only up to 1 ms. In this time domain O just started to accumulate (Fig. 5). At $\sim$10 ms, where intermediate O reaches its maximum, the RC of the system already dominates their signal. This explains why they could not observe any electric signal related to the last part of the photocycle, and why the analysis we report here disagrees with the conclusion of these authors that the O intermediate is not part of the chloride-transporting photocycle.

Although the electric signals of the *pharaonis* halorhodopsin-containing oriented gel samples were very small, a good correlation could be established between the electric signals and the photocycle steps. The electrogenicities of the intermediates in the chloride-transporting photocycle were calculated. They clearly identify the steps when the ion moves across the membrane during its transport.

The authors are grateful to Prof. L. Keszthelyi and Dr. A. Dér for helpful discussions.

This work was supported by National Science Research Fund of Hungary Grant OTKA T022066 and the Academic Research Fund of the Hungarian Academy of Sciences Grant 97-71, 3, 3/52 (to G.V.), and National Institutes of Health Grant GM 29498 (to J.K.L.).

REFERENCES

Balashov, S. P., E. S., Imasheva, R. Govindjee, and T. G. Ebrey. 1996. Titration of aspartate-85 in bacteriorhodopsin: what it says about chromophore isomerization and proton release. *Biophys. J.* 70:473–481.

Bamberg, E., N. A. Dencher, A. Fahr, and M. P. Heyn. 1981. Transmembranous incorporation of photoelectrically active bacteriorhodopsin in planar lipid bilayers. *Proc. Natl. Acad. Sci. USA.* 78:7502–7506.

Bamberg, E., P. Hegemann, and D. Oesterhelt. 1984. The chromoprotein of halorhodopsin is the light-driven electrogenic chloride pump in *Halobacterium halobium. Biochemistry.* 23:6216–6221.

Bivin, D. B., and W. Stoeckenius. 1986. Photoactive retinal pigments in haloalkalophilic bacteria. *J. Gen. Microbiol.* 132:2167–2177.

Blanck, A., and D. Oesterhelt. 1987. The halorhodopsin gene II. Sequence, primary structure of halorhodopsin, and comparison with bacteriorhodopsin. *EMBO J.* 6:265–273.

Braiman, M. S., T. J. Walter, and D. M. Briercheck. 1994. Infrared spectroscopic detection of light-induced change in chloride-arginine interaction in halorhodopsin. *Biochemistry.* 33:1629–1635.

Butt, H.-J., K. Fendler, E. Bamberg, J. Tittor, and D. Oesterhelt. 1989. Aspartic acids 96 and 85 play a central role in the function of bacteriorhodopsin as a proton pump. *EMBO J.* 8:1657–1663.

Dér, A., K. Fendler, L. Keszthelyi, and E. Bamberg. 1985b. Primary charge separation in halorhodopsin. *FEBS Lett.* 187:233–236.

Dér, A., P. Hargittai, and J. Simon. 1985a. Time-resolved photoelectric and absorption signals from oriented purple membranes immobilized in gel. *J. Biochem. Biophys. Methods.* 10:295–300.

Dér, A., R. Tóth-Boconádi, and S. Száraz. 1992. Electric signals and the photocycle of bacteriorhodopsin. *In* Structures and Functions of Retinal Proteins. J. L. Rigaud, editor. John Libbey and Co., London. 197–200.

Drachev, L. A., A. D. Kaulen, L. V. Khitrina, and V. P. Skulachev. 1981. Fast stages of photoelectric processes in biological membranes. I. Bacteriorhodopsin. *Eur. J. Biochem.* 117:461–470.

Gergely, C., C. Ganea, G. I. Groma, and G. Váró. 1993. Study of the photocycle and charge motions of the bacteriorhodopsin mutant D96N. *Biophys. J.* 65:2478–2483.

Gerscher, S., M. Mylrajan, P. Hildebrandt, M. H. Baron, R. Müller, and M. Engelhard. 1997. Chromophore-anion interaction in halorhodopsin from *Natronobacterium pharaonis* probed by time-resolved resonance Raman spectroscopy. *Biochemistry.* 36:11012–11020.

Havelka, W. A., R. Henderson, and D. Oesterhelt. 1995. Three-dimensional structure of halorhodopsin at 7 Å resolution. *J. Mol. Biol.* 247:726–738.

Holz, M., M. Lindau, and M. P. Heyn. 1988. Distributed kinetics of the charge movements in bacteriorhodopsin: evidence for conformational substates. *Biophys. J.* 53:623–633.

Ihara, K., T. Umemura, I. Katagiri, T. Kitajima-Ihara, Y. Sugiyama, Y. Kimura, and Y. Mukohata. 1999. Evolution of the archaeal rhodopsins: evolution rate changes by gene duplication and functional differentiation. *J. Mol. Biol.* 285:163–174.

Kalaidzidis, I. V., Y. L. Kalaidzidis, and A. D. Kaulen. 1998. Flash-induced voltage changes in halorhodopsin from *Natronobacterium pharaonis. FEBS Lett.* 427:59–63.

Keszthelyi, L., and P. Ormos. 1980. Electric signals associated with the photocycle of bacteriorhodopsin. *FEBS Lett.* 109:189–193.

Lanyi, J. K. 1986. Halorhodopsin: a light-driven chloride pump. *Annu. Rev. Biophys. Biophys. Chem.* 15:11–28.

Lanyi, J. K. 1990. Halorhodopsin: a light-driven electrogenic chloride transport system. *Physiol. Rev.* 70:319–330.

Lanyi, J. K., A. Duschl, G. W. Hatfield, K. M. May, and D. Oesterhelt. 1990b. The primary structure of a halorhodopsin from *Natronobacterium pharaonis*: structural, functional and evolutionary implications for bacterial rhodopsins and halorhodopsins. *J. Biol. Chem.* 265:1253–1260.

Lanyi, J. K., A. Duschl, G. Váró, and L. Zimányi. 1990a. Anion binding to the chloride pump, halorhodopsin, and its implications for the transport mechanism. *FEBS Lett.* 265:1–6.

Ludmann, K., C. Gergely, A. Dér, and G. Váró. 1998a. Electric signals during the bacteriorhodopsin photocycle, determined over a wide pH range. *Biophys. J.* 75:3120–3126.

Ludmann, K., C. Gergely, and G. Váró. 1998b. Kinetic and thermodynamic study of the bacteriorhodopsin photocycle over a wide pH range. *Biophys. J.* 75:3110–3119.

Matsuno-Yagi, A., and Y. Mukohata. 1980. ATP synthesis linked to light-dependent proton uptake in a red mutant strain of Halobacterium lacking bacteriorhodopsin. *Arch. Biochem. Biophys.* 199:297–303.

Muneyuki, E., C. Shibazaki, H. Ohtani, D. Okuno, M. Asaumi, and T. Mogi. 1999. Time-resolved measurements of photovoltage generation by bacteriorhodopsin and halorhodopsin adsorbed on a thin polymer film. *J. Biochem.* 125:270–276.

Oesterhelt, D. 1995. Structure and function in halorhodopsin. *Israel J. Chem.* 35:475–494.

Oesterhelt, D., and J. Tittor. 1989. Two pumps, one principle: light-driven ion transport in halobacteria. *TIBS.* 14:57–61.

Okuno, D., M. Asaumi, and E. Muneyuki. 1999. Chloride concentration dependency of the electrogenic activity of halorhodopsin. *Biochemistry.* 38:5422–5429.

Otomo, J., H. Tomioka, and H. Sasabe. 1992. Properties and the primary structure of a new halorhodopsin from halobacterial strain mex. *Biochim. Biophys. Acta Bio-Membr.* 1112:7–13.

Rüdiger, M., and D. Oesterhelt. 1997. Specific arginine and threonine residues control anion binding and transport in the light-driven chloride pump halorhodopsin. *EMBO J.* 16:3813–3821.

Scharf, B., and M. Engelhard. 1994. Blue halorhodopsin from *Natronobacterium pharaonis*: wavelength regulation by anions. *Biochemistry.* 33: 6387–6393.

Schobert, B., and J. K. Lanyi. 1982. Halorhodopsin is a light-driven chloride pump. *J. Biol. Chem.* 257:10306–10313.

Soppa, J., J. Duschl, and D. Oesterhelt. 1993. Bacterioopsin, haloopsin, and sensory opsin I of the halobacterial isolate *Halobacterium* sp. strain SG1: three new members of a growing family. *J. Bacteriol.* 175: 2720–2726.

Trissl, H. W. 1990. Photoelectric measurements of purple membranes. *Photochem. Photobiol.* 51:793–818.

Váró, G., L. S. Brown, H. Sasaki, H. Kandori, A. Maeda, R. Needleman, and J. K. Lanyi. 1995b. Light-driven chloride ion transport by halorhodopsin from *Natronobacterium pharaonis* 1. The photochemical cycle. *Biochemistry.* 34:14490–14499.

Váró, G., R. Needleman, and J. K. Lanyi. 1995a. Light-driven chloride ion transport by Halorhodopsin from *Natronobacterium pharaonis*. 2. Chloride release and uptake, protein conformation change, and thermodynamics. *Biochemistry.* 34:14500–14507.

Váró, G., L. Zimányi, X. Fan, L. Sun, R. Needleman, and J. K. Lanyi. 1995c. The photocycle of halorhodopsin from *Halobacterium salinarum*. *Biophys. J.* 68:2062–2072.

Zimányi, L., and J. K. Lanyi. 1993. Deriving the intermediate spectra and photocycle kinetics from time-resolved difference spectra of bacteriorhodopsin. The simpler case of the recombinant D96N protein. *Biophys. J.* 64:240–251.